



HAL
open science

Development of a microfluidic droplet platform with an antibody-free magnetic-bead-based strategy for high through-put and efficient EVs isolation

Marco Morani, Myriam Taverna, Zuzana Krupova, Lucile Alexandre, Pierre Defrenaix, Thanh Duc Mai

► To cite this version:

Marco Morani, Myriam Taverna, Zuzana Krupova, Lucile Alexandre, Pierre Defrenaix, et al.. Development of a microfluidic droplet platform with an antibody-free magnetic-bead-based strategy for high through-put and efficient EVs isolation. *Talanta*, 2022, 249, pp.123625. 10.1016/j.talanta.2022.123625 . hal-03841027

HAL Id: hal-03841027

<https://hal.science/hal-03841027>

Submitted on 22 Jul 2024

HAL is a multi-disciplinary open access archive for the deposit and dissemination of scientific research documents, whether they are published or not. The documents may come from teaching and research institutions in France or abroad, or from public or private research centers.

L'archive ouverte pluridisciplinaire **HAL**, est destinée au dépôt et à la diffusion de documents scientifiques de niveau recherche, publiés ou non, émanant des établissements d'enseignement et de recherche français ou étrangers, des laboratoires publics ou privés.



Distributed under a Creative Commons Attribution - NonCommercial - NoDerivatives 4.0 International License

1 **Development of a microfluidic droplet platform with an antibody-free magnetic-bead-**
2 **based strategy for high through-put and efficient EVs isolation**

3

4 **Marco Morani¹, Myriam Taverna^{1,2}, Zuzana Krupova³, Lucile Alexandre¹, Pierre**
5 **Defrenaix³, and Thanh Duc Mai^{1*}**

6

7 ¹ *Université Paris-Saclay, CNRS, Institut Galien Paris-Saclay, 92296, Châtenay-Malabry,*
8 *France.*

9 ² *Institut Universitaire de France (IUF)*

10 ³ *Excilone - 6, Rue Blaise Pascal - Parc Euclide - 78990 Elancourt - France*

11

12 **Correspondence:** E-mail: thanh-duc.mai@u-psud.fr

13

14

15 **Keywords:** extracellular vesicles; isolation; magnetic beads; polymer precipitation;
16 microfluidic droplets

17

18

19

20

21

22

23

24

25

26 **Abstract**

27 In this study, we present a novel microfluidic droplet-based strategy for high performance
28 isolation of extracellular vesicles (EVs). For EVs capture and release, a magnetic bead-based
29 approach without having recourse to any antibody was optimized in batch and then adapted to
30 the microfluidic droplet system. This antibody-free capture approach relies on the presence of
31 a water-excluding polymer, polyethylene glycol (PEG), to precipitate EVs on the surface of
32 negatively charged magnetic beads. We significantly improved the reproducibility of EV
33 recovery and avoided positive false bias by including a washing step and optimizing the
34 protocol. Well-characterized EV standards derived from pre-purified bovine milk were used
35 for EVs isolation performance evaluation. An EVs recovery of up to 25 % estimated with
36 nanoparticle tracking analysis (NTA) was achieved for this batchwise PEG-based approach.
37 The confirmation of isolated EVs identity was also made with our recently developed method
38 using capillary electrophoresis (CE) coupled with laser-induced fluorescent (LIF) detection.
39 In parallel, a purpose-made droplet platform working with magnetic tweezers was developed
40 for translation of this PEG-based method into a droplet microfluidic protocol to further
41 improve the performance in terms of EVs capture efficiency and high throughput. The
42 droplet-based protocol offers a significant improvement of recovery rate (up to 50 %) while
43 reducing sample and reagent volumes (by more than 10 folds) and operation time (by 3 folds)
44 compared to the batch-wise mode.

45

46

47

48

49

50

51 **1. Introduction**

52 Extracellular vesicles (EVs) are phospholipid bilayer-delimited particles produced by most
53 cell types and present in many body fluids [1, 2]. EVs contain and carry diverse biomolecules
54 that are specific to the mother cells from which they are secreted, allowing them to transmit a
55 variety of essential signals under both normal and pathological conditions. Hence, the
56 potential of EVs as prognostic or diagnostic biomarkers has attracted significant attention in
57 recent years [3, 4]. Furthermore, due to their high specific targeting ability, EVs have gained
58 much interest as engineered drug delivery systems for clinical and pharmaceutical
59 applications [5, 6]. However, there are still technological hurdles to purify, analyze and
60 characterize such nanometric bio-entities. Many methods for isolating EVs have been
61 developed so far, including ultracentrifugation (UC), gradient ultracentrifugation,
62 ultrafiltration (UF), polymer co-precipitation, size-exclusion liquid chromatography (SEC),
63 immuno-extraction [7]. Among these, ultracentrifugation is widely considered as the gold
64 standard in all EV applications. However, this technique presents many drawbacks, such as
65 time-consuming procedures, contamination of EV populations by protein aggregates and other
66 particles, damage to the EVs membrane structure and possible considerable loss of EVs (EVs
67 yield may drop to 2 %) [8, 9]. Thus, there is still an urgent need for emerging EVs isolation
68 approaches that can provide EV purity and integrity in a reproducible and high-throughput
69 manner. Many modern isolation methods have been developed in this direction, such as flow
70 field-flow fractionation, ion-exchange, electrokinetic approaches as well as the combination
71 of multiple techniques, like UC with UF or SEC [10-12]. In parallel, microfluidic
72 technologies have made significant progresses for such purpose, exploiting both physical and
73 biochemical properties of EVs at micro/nanoscale level for their capture and/or detection [13-
74 17]. The majority of microfluidic approaches rely on immunoaffinity to selectively capture
75 EVs. Immunoaffinity bead-based kits allow highly selective isolation of EVs through

76 antibodies specific for target EVs surface proteins [18-20]. However, following isolation,
77 those commercial kits, which are rather used for subsequent EVs downstream lysis and
78 analysis, do not provide any efficient elution possibility to recover intact EVs. Moreover, the
79 main disadvantage of those strategies is the absence of universal EVs markers to ensure total
80 capture of all EVs. Few recent works on capture and eventual elution of EVs on magnetic
81 beads have been reported, using either electrostatic interaction [21], polymer mediated
82 adsorption of EVs on magnetic beads [22], a DNA aptamer-based system [23] or DNA linker
83 spacers [24]. No EVs recovery efficiency was reported in these works that used cell culture
84 media and/or plasma samples as starting materials from which accurate EVs quantification is
85 not trivial. At the actual stage, these works had to be realized batchwise with multiple in-tube
86 steps without automation.

87

88 The goal of this study was to investigate bead-based strategies for isolating and recovering
89 intact EVs without the use of immunoaffinity recognition and to adapt them to droplet
90 microfluidics. For such purposes, well-characterized high-quality EVs isolated from bovine
91 milk were used as EVs standards rather than non-quantified EVs from cell culture and plasma
92 samples. Then, the batchwise approach with the superior performance was transferred into an
93 automated and high-throughput protocol relying on a microfluidic droplet train. Different
94 operations in microfluidic droplets were developed and optimized to overcome the challenges
95 of beads clustering and poor recirculation in droplets in the presence of viscous polymers,
96 allowing to realise EVs capture on beads, washing and elution with a droplet sequence. So far,
97 droplet microfluidics has been communicated only twice for immunoassay-based detection of
98 EVs [25, 26] and has never been exploited for high performance and high throughput isolation
99 of EVs.

100

101 **2. Materials and methods**

102 **2.1. Chemicals and reagents**

103 2-(cyclohexylamino)ethanesulfonic acid (CHES), phosphate buffered saline (PBS 10x),
104 sodium dodecyl sulfate (SDS, 98.5 % (GC)), tris(hydroxymethyl)aminomethane (Tris),
105 polyethylene glycol (PEG 8000), albumin from human serum, IgG from human serum and
106 human transferrin were all obtained from Sigma Aldrich (St. Louis, MO, USA). Sodium
107 hydroxide (1 M) and hydrochloric acid (1 M) were obtained from VWR (Fontenay-sous-Bois,
108 France). All solutions were prepared with deionized water purified with a Direct - Q3 UV
109 purification system (Millipore, Milford, MA, USA). Vybrant™ CFDA SE Cell Tracer Kit
110 (dye 5-(and-6)-carboxyfluorescein diacetate succinimidyl ester, CFDA-SE) was purchased
111 from Thermo Fisher Scientific (Waltham, MA, USA). Fluorinert oil FC-40 (ZF-0002-1308-0)
112 was purchased from 3 M (USA). The surfactant 1H, 1H, 2H, 2H – perfluoro-1-decanol was
113 obtained from Sigma Aldrich. ExoCAS-2 kit containing poly-L-lysine-coated magnetic beads,
114 washing and elution buffer solutions was purchased from Microgentas (Seongbuk-gu,
115 Republic of Korea). Carboxylate functionalized magnetic beads (Dynabeads MyOne, 10
116 mg/mL, diameter of 1 µm) and silica-based magnetic beads (Dynabeads MyOne Silane, 40
117 mg/mL, diameter of 1 µm) were obtained from Thermo Fisher Scientific. EVs samples
118 isolated from bovine milk were provided by Excilone (Elancourt, France).

119

120 **2.2. Apparatus and material**

121 For macroscale protocols, all magnetic-bead-based assays in batch were carried out in protein
122 LoBind 1.5 mL tubes purchased from Eppendorf (Hamburg, Germany). For retaining
123 magnetic beads, a neodymium magnet purchased from Ademtech (Adem Mag MSV, Bessac,
124 France) was used. Shaking of magnetic bead suspensions during the incubation and washing
125 steps was realized with a mixer (Eppendorf ThermoMixer C).

126 For droplet microfluidic operations, a microfluidic droplet platform was constructed and was
127 inspired from our previous configuration [27]. It comprises a syringe pump (from Nemesys,
128 Cetoni GmbH) equipped with 1 mL glass syringes (purchased from SGE) and a motorized
129 pipettor arm (Rotaxys, Cetoni GmbH), used for droplets generation. A 96-well plate (Thermo
130 Scientific) was used for sample storage and reagent solutions. The plate was mounted on a
131 custom-made holder that can be moved in the X, Y, and Z directions. PTFE tubing with ID of
132 0.3 mm and OD of 0.6 mm (Z609692-1PAK, Sigma Aldrich) was used to conduct the droplet
133 trains. Fluorinated oil FC-40 mixed with the surfactant (1H, 1H, 2H, 2H – perfluoro-1-
134 decanol, 2 % w/w) was used to separate aqueous droplets inside PTFE tubing. In the protocol,
135 a magnetic tweezer, prepared in-house was used. It is composed of a paramagnetic tip
136 activated by a magnetic coil. Macro Objective (MLH-10X) mounted on a low-cost CMOS
137 Cameras (acA1300-60 gm, Basler) and white LED back light illumination (Schott Lighting
138 and Imaging) were employed for droplet observation.

139

140 The analyses using CE coupled with laser induced fluorescent detection (CE-LIF) were
141 performed with a PA 800 Plus system (Sciex Separation, Brea, CA) equipped with a solid-
142 state LIF detector (excitation wavelength of 488 nm, emission wavelength of 520 nm)
143 purchased from Integrated Optics (Art. No. 40A-48A-52A-64A-14-DM-PT, distributed by
144 Acal BFi, Evry, France). Uncoated fused silica capillaries were purchased from CM Scientific
145 (Silsden,UK). Data acquisition and instrument control were carried out using Karat 8.0
146 software (Sciex Separation, Brea, CA).

147

148 **2.3. Methods**

149 *Isolation of bovine milk-derived EVs with sucrose gradient ultracentrifugation*

150 Skimmed bovine milk samples were obtained by centrifugation of 50 mL whole milk at 3000
151 g for 30 min at 4 °C (Allegra X-15R, Beckman Coulter, France). The whey was obtained after
152 acid precipitation with 10 % (v/v) acetic acid, incubation at 37 °C for 10 min and 10 % (v/v)
153 1M sodium acetate for 10 min at RT followed by centrifugation at 1500 g, 4 °C for 15 min
154 and filtration using vacuum-driven filtration system Millipore Steritop, 0.22 µm. The whey
155 supernatants were concentrated using Amicon 100 kDa centrifugal filter units (Merck
156 Millipore) at 4000 g and 20 °C up to final volume of 6 mL. The obtained retentate was ultra-
157 centrifuged for pelleting the EVs at 100000 g for 70 min at 4°C (Beckman Coulter, Optima
158 XPN-80, 50TI rotor). The pellets were solubilized in 500 µL of PBS then added to 11 mL of
159 pre-prepared sucrose gradient 5-40 % and ultra-centrifuged at 200000 g for 18 h at 4 °C
160 (Beckman Coulter, Optima XPN-80, SW41 rotor). Fractions of 1 mL were collected and the
161 selected ones containing targeted exosome population were diluted in 6 mL of PBS 1X and
162 finally centrifuged at 100000 g for 70 min at 4 °C (Beckman Coulter, Optima XPN-80, 50TI
163 rotor). The pellets were resuspended in 50 µL of PBS 1X and stored at -80 °C, until further
164 analyses.

165

166 *Isolation of pony plasma and serum derived EVs with size exclusion chromatography (SEC)*

167 Preparation of plasma: Peripheral blood was collected into EDTA-coated vacutainer tubes.
168 After ten-time inversion, samples were processed within the 60 min of collection. Consecutive
169 centrifugation steps at 2500 g, 4 °C for 15 min and then at 15000 g for 10 min were performed
170 followed by filtration of the supernatant through 0.22 µm filters. Preparation of serum: Whole
171 blood was collected into anticoagulant-free tubes and allowed to clot at room temperature for
172 45 min. The clot was removed by centrifugation at 3200 g, 4 °C for 15 min, followed by
173 centrifugation at 15000 g, 4 °C for 10 min and filtration of the supernatant through 0.22 µm
174 filters. 500 µL of pre-treated plasma/serum was loaded onto a qEVoriginal SEC column (Izon

175 Science, New Zealand) previously washed and equilibrated with PBS. Fraction collection
176 (0.5 mL per fraction) was carried out immediately using PBS 1X as elution buffer. The
177 selected elution fractions were pooled and subsequently concentrated using 100 kDa Amicon
178 centrifugal filter units (Merck Millipore). Post-treatment processing with several washing
179 steps with PBS was applied to obtain pure EV fractions that are highly enriched with
180 exosomes.

181

182 *EV isolation using commercial kits*

183 ExoCAS-2 magnetic bead-based ion exchange kit was used for the study of EV yield
184 performance. The experimental procedure is described in a paper recently published [21].
185 Briefly, PLL-coated beads were mixed with our standard EVs (bovine milk derived EVs),
186 followed by incubation of the mixture for 30 min at 4 °C in a rocking mixer. After incubation,
187 the EVs-bound beads were carefully washed with 2 mL of ExoCAS-2 washing solution and
188 then re-suspended in ExoCAS-2 elution solution by shaking for 5 min at 1000 rpm. Finally, a
189 magnet was employed to retain magnetic beads and the supernatant containing yielded EVs
190 was collected.

191

192 *PEG-based EVs precipitation on magnetic beads in batch mode*

193 For PEG-based EVs precipitation on magnetic beads in batch, a volume of 200 µL of PEG
194 (25 % m/v), 150 µL of carboxylate functionalized magnetic beads (10 mg/mL) and 250 µL of
195 deionized water was incubated with 400 µL of standard EVs or biological fluid (simulated
196 human serum and pony plasma and serum, 5 times diluted with deionized water) on a mixer at
197 25 ° C for 1 h at 700 rpm. Beads were then carefully washed twice with PEG 5 % / NaCl 0.2
198 M. After removal of washing solution, the magnetic beads in tubes were re-dispersed in 400

199 μ L of PBS 1X solution and then incubated on shaking for 5 min at 25 °C for EV elution. A
200 magnet was used to remove the magnetic beads, and EVs were recovered in the supernatant.

201

202 *PEG-based EVs precipitation on magnetic beads using the microfluidic droplet platform*

203 A robotic arm and a 500 μ L syringe were utilized to pipette the droplets from separate
204 reservoirs into a PTFE tube in a fully automated manner. To complete one PEG-based EVs
205 precipitation protocol, a train of 5 droplets (each containing 6 μ L) confined and separated by
206 oil was required. It includes: i) one droplet of carboxylate functionalized magnetic beads (1.5
207 mg/mL), ii) one droplet of EV sample in PEG 5 %, iii-iv) two droplets of washing solution
208 (PEG 5 % / NaCl 0.2 M) and v) one droplet of elution solution (PBS 1X). Beads were trapped
209 out of one droplet and released into another by electronic triggering of the magnetic tweezer.
210 The incubation was carried out with regular droplet back and forth movements at RT for 25
211 min. After incubation, two washing droplets are flushed over EVs-bound beads. The EVs-
212 bound beads were then dispersed into the elution droplet with regular droplet back and forth
213 movements at RT for 5 min. The elution droplet containing released EVs was then collected
214 in a tube for downstream analysis.

215

216 *Nanoparticle Tracking Analysis (NTA) of EVs*

217 Particle concentration and size distribution were determined with a Nanosight NS300
218 instrument (Malvern, version NTA 3.2 Dev Build 3.2.16) equipped with a 405 nm laser,
219 sCMOS camera type and the NTA software v3.1. The video acquisition was performed using
220 a camera level of 14. 3 videos of 90 s with a frame rate of 30 frames/s were captured for each
221 sample at 25 °C and subsequently analyzed with a threshold set up at 5. The results were
222 validated with at least 2000 valid tracks for each triplicate. All experiments were carried out
223 with samples pre-diluted in PBS according to input sample concentrations. The working

224 particle concentrations were kept within the range of 10^6 - 10^9 particles per mL for optimal
225 analysis.

226

227 The Zetaview system (Particle Metrix, Germany) was equipped with a 488 nm laser. EVs
228 samples were diluted to allow the measurements at 50–200 particles/frame. Each experiment
229 was performed in duplicate on 11 different positions within the sample cell. The
230 specifications used for all measurements were cell temperature of 25 °C, sensitivity of 70,
231 shutter of 100, Max Area of 1000, Min Area of 10, Min Brightness of 25. The results were
232 validated with at least 1000 valid tracks for each run. For data capture and analysis, the
233 Nanoparticle Tracking Analysis Software (ZNTA) vs 8.05.04 was used.

234

235 *CE-LIF of fluorescently labelled EVs*

236 Details on the CE-LIF method for EVs analysis can be seen in our recent work [28]. Briefly,
237 fluorescently labelled EVs were prepared using the 5-(and-6)-carboxyfluorescein diacetate
238 succinimidyl ester (CFDA-SE). After removal of residual CFDA-SE via filtration with
239 commercial Exosome Spin Columns (MW 3000, Thermo Fisher Scientific Waltham, MA
240 USA), labelled EVs were analyzed with CE-LIF using a fused silica capillary having I.D. of
241 50 μm , effective length (L_{eff}) of 50.2 cm and total length (L_{tot}) of 60.2 cm. The capillary was
242 pre-conditioned with water for 10 min, 1 M NaOH for 10 min, 1 M HCl for 10 min and then
243 water for 10 min. The rinsing between two analyses was carried out with 50 mM SDS for 5
244 min, 1 M NaOH for 5 min, deionized water for 5 min, and finally the running BGE composed
245 of Tris / CHES (IS 90 mM, pH 8.4) for 5 min using a pressure of 30 psi. EVs samples were
246 injected hydrodynamically from the inlet end by applying a pressure of 0.5 psi for 2 min. The
247 separation was carried out under 25 kV (normal polarity) at 25 °C and the samples were kept
248 at 5 °C with the sample storage module of the PA 800 Plus equipment.

249

250 **3. Results and discussion**

251 **3.1. Batchwise EVs isolation development**

252 With the aim to establish a high-performance and high-throughput microfluidic droplet
253 system for EVs isolation, we evaluated two recently communicated batchwise EV-enrichment
254 strategies that are alternative approaches to the immunoaffinity-based ones. They hold high
255 potential for subsequent translation into a microfluidic format in terms of minimal forefront
256 preparations, non-laborious operations, as well as ease of manipulation and step transition
257 thanks to the use of magnetic beads as cargos. The first one is a magnetic bead-mediated
258 selective adsorption strategy (MagExo), exploiting the presence of a water-excluding
259 polymer, polyethylene glycol (PEG), to lock up a significant number of water molecules,
260 forcing thereby the EVs to aggregate and precipitate on the surface of magnetic beads [22].
261 The second strategy called ExoCAS-2 relies on an ionic exchange mechanism, using magnetic
262 beads coated with a polycationic polymer, poly-L-lysine (PLL), to quickly trap negatively
263 charged EVs via electrostatic interaction [21]. For performance comparison, EVs standards
264 derived from bovine milk having narrow size distribution, with well-defined concentrations
265 and exhaustive characterizations by NTA, DLS, LC-MS/MS and TEM, were used as the
266 starting sample. TEM images revealed the absence of contaminating protein residues in these
267 EVs standards (Fig. S1A in the supporting information ESI). Major protein contaminants (e.g.
268 α -s1 casein, β -casein, α -Lactalbumin and serum albumin) were not found according to the
269 LC-MS/MS analysis (Fig. S1B). The use of EV standards of high purity allowed to evaluate
270 the EVs recovery more accurately. In our case, quantification of EVs isolation yields obtained
271 with MagExo and ExoCAS-2 methods was possible by comparing the EVs concentrations
272 before and after isolation processes (see Fig. 1). Unsatisfactory EVs recovery (less than 10 %)
273 was obtained with commercial PLL-coated beads, compared to that achieved when using PEG

274 and silica magnetic beads (34 %). NTA data also showed a size shift towards smaller particles
275 when EVs were eluted from PLL beads. This could be a consequence of PLL release from the
276 beads during the elution process. This was confirmed by the CE-LIF analysis (discussion
277 below). This led to a critical PLL concentration in the eluent that is high enough to cause EVs
278 lysis. Indeed, several studies have shown that PLL can penetrate through vesicles via
279 interaction with the lipid membrane [29-31], provoking vesicle lysis from a certain threshold
280 concentration of PLL [32]. In parallel to NTA measurements for EVs recovery evaluation, we
281 used our recently developed CE-LIF approach [28] to validate the identity of EVs collected
282 with MagExo and ExoCAS-2 methods (see Fig. 2). The peak profile of EVs collected with
283 PEG-based protocol corresponds well to the fingerprint of bovine milk-derived EVs,
284 confirming the presence of intact EVs in the eluent (Fig. 2A). On the contrary, with the ion
285 exchange method, multiple tagged species were detected. To understand the origin of these
286 peaks, solutions containing different PLL concentrations without the presence of EVs were
287 analyzed. As can be seen in Fig. 2B, many peaks were still detected, whose intensities were
288 related to the PLL concentrations. These results confirmed the hypotheses that the peaks
289 observed come from PLL leakage from the magnetic beads, which could not be visualized
290 with conventional NTA. The released PLL which can be labelled by the residual CFDA-SE
291 dye through its amino groups lead to unwanted products in the eluent. The ExoCAS-2 method
292 was therefore not further considered; and the PEG-based method (MagExo) was chosen for
293 further optimisation.

294

295 Besides the preservation of intact EVs after purification, protocol reproducibility is another
296 important point to consider to guarantee consistency of isolated EVs population and quality.
297 Indeed, by reproducing the MagExo procedure described in reference [22], we observed
298 significant batch-to-batch variation in vesicle concentration (RSD of 30 %). The lack of EVs

299 washing between the capture and elution steps in the original protocol led to misleading data.
300 To minimize this cross contamination and to recover intact EVs for further characterization,
301 we developed a washing protocol after the EVs capture step. By adding two consecutive
302 washing steps with PEG 5 % w/v to remove residual unbound EVs while maintaining
303 captured EVs on magnetic beads, we significantly improved the repeatability (RSD) to 8 %.
304 This came with some penalty, as the EV isolation yield fell to 17 %. To further improve the
305 performance of EVs capture and thus isolation yield, we carried out different optimizations on
306 magnetic bead concentrations (0.5 – 2 mg/mL), bead chemical surface (with carboxylic or
307 silane groups), incubation temperature for EVs capture (4 – 25 °C) as well as PEG
308 concentrations (5-15 % w/v). Note again that the performance of EVs capture relies on the
309 presence of PEG to force the EVs to precipitate (by locking up a significant number of water
310 molecules) on the surface of magnetic beads. As can be seen in Fig. S2 in the ESI, much
311 better EVs capture performance was achieved with beads with carboxylic groups (EVs yield
312 of 61 %) than with silane groups (less than 5 %). The incubation temperature was found not to
313 significantly influence the EVs capture performance, with no remarkable difference
314 observed at 4 °C (yield of 17.2 %) and 25 °C (yield of 20 %). The concentrations of magnetic
315 beads and PEG played important roles in the on-bead retaining of EVs. A compromise of their
316 concentrations had to be made to allow facile PEG-induced precipitation of EVs on sufficient
317 quantity of carboxylate beads, while avoiding i) poor recirculation or even clustering of beads
318 at too high concentrations and ii) hinderance of the arrival of EVs on to the beads surface due
319 to too elevated medium's viscosity at too high PEG concentrations. Overall, the highest EVs
320 recovery rate (after 2 washing steps) of 25 % \pm 8 % was achieved with the optimized
321 conditions using PEG concentration of 5 % and carboxylic magnetic beads' concentration of
322 1.5 mg/mL with 1 h incubation at 25 °C. A higher bead concentration of 2 mg/mL was tested
323 but no satisfactory results were obtained due to clustering and poor circulation of beads. PEG

324 concentrations lower than 5 % w/v were not considered in our work, based on previous
325 optimization already reported [22]. Conveniently, the working temperature of 25 °C is well
326 adapted for subsequent translation of batchwise protocol into a microfluidic format where
327 cooling function is not readily available. To evaluate the reusability of magnetic beads
328 functionalized with carboxylic groups for repeated isolation of EVs, the same beads employed
329 for the first round of capture and elution of EVs were recovered in PBS and then subjected to
330 the second and third rounds. As shown in Fig. S3 in the ESI, the concentration range of
331 recovered EVs in the second round is similar to that obtained from the first round. The
332 variation of recovered EVs concentrations is however significantly higher (RSD of 24 % vs. 9
333 %, respectively). While the surface charge of the beads is expected not to be hammered by the
334 elution media (i.e., PBS), the possible presence of residual PEG on the surface of beads after
335 the first elution step could explain such an elevated variation in the second round. When using
336 the same beads for the third cycle of EVs capture – elution, no satisfactory results were
337 obtained, with the recovered EVs concentration almost 5-fold lower than those obtained in
338 previous cycles (Fig. S3 in ESI). While the reusability of magnetic beads for EVs capture and
339 elution is possible for 2 cycles with careful consideration of PEG presence, fresh beads
340 without recycling are nevertheless required for further experiments in order to minimize the
341 risk of EVs isolation uncertainty.

342

343 **3.2. Droplet microfluidics for EVs isolation: proof of concept**

344 The optimised batchwise PEG-based method was subsequently converted into a microfluidic
345 droplet protocol in order to provide a high level of automation and integration, significant
346 reduction in sample/reagent amounts, and a higher performance in terms of isolation
347 efficiency. The instrumental setup of the purpose-made microfluidic platform is shown in Fig.
348 3. It is composed of a syringe pump, a motorized pipettor arm for droplet production, a 96-

349 well plate for sample and reagent storage and a magnetic tweezer for manipulation of
350 magnetic beads. With this system, we used a train of 6 μ L droplets containing in a defined
351 sequence (i) the magnetic bead suspension, (ii) the EVs sample, (iii) the washing and (iv)
352 elution solutions to replace different tube-based steps. When working with the droplet-wise
353 multi-step protocol, one hurdle encountered is the difficulty to efficiently transfer the target
354 species (EVs in this case) from one droplet to another without any risk of cross
355 contamination. This was expected to be overcome with our setup through the use of magnetic
356 beads as the controllable carrier of target analytes between droplets. A purpose-made
357 magnetic tweezer, composed of a paramagnetic tip activated by an electrical coil [27, 33], was
358 employed to manipulate magnetic beads between droplets via application of an external
359 electrical field. Table 1 provides an overview of the operation sequence. A train of droplets
360 containing different solutions and sample in a defined order was delivered through the
361 magnetic tweezer where the beads were extracted from the first droplet and transported into
362 the sample one containing EVs. The incubation was subsequently performed by pushing the
363 droplet train back and forth inside the tubing. The magnetic beads that retain EVs on their
364 surface were then trapped by the magnetic tweezer and the supernatant droplet was washed
365 away, followed by flushing of the trapped magnetic beads with two washing droplets. The
366 washed beads were finally released into an elution droplet that was finally collected in an oil-
367 containing tube for further analyses.

368

369 Several problems were however encountered that led to failure of such droplet protocol in our
370 first experiments, notably beads clustering and poor recirculation in droplets in the presence
371 of PEG. Indeed, the beads often stayed at the rear of the moving droplet, forming undesired
372 bead clusters when the droplet moved inside the tubing over an extended distance. This was
373 ascribed to come from the presence of PEG which significantly increased droplet viscosity

374 [34], which in turn impaired the effective recirculation of the beads (see Fig. S4 in the ESI).
375 To enhance recirculation of the beads within a droplet, we put our efforts on optimizing the
376 droplet movement pattern and travel volume (i.e., the oil volume required to push and pull the
377 droplet) during the back-and-forth movement. Chaotic trajectories are known to enhance
378 mixing efficiency [35, 36]. Consequently, different droplet movement patterns were also
379 tested, including the straight, the U-shaped patterns (i.e., the tubing was shaped over a
380 metallic guideline) and the spiral-formed one (i.e., the tubing was coiled around a cylindrical
381 support) (see Fig. S5 in ESI). With the straight pattern, bead aggregation was always observed
382 in the presence of PEG, regardless of the travel volume (Fig. S4A). For other movement
383 patterns, bead clustering was alleviated but still visible when working with a large travel
384 volume of 10 μ L (Fig. S4 B and C). This undesired phenomenon was finally avoided when
385 employing the spiral or U-shaped patterns with a short travel volume of 6 μ L (equivalent to a
386 droplet volume). By keeping these optimized setups and conditions, we further investigated
387 the in-droplet incubation duration (from 5 to 45 min) during the EVs capture step (Fig. S6 in
388 the ESI). The EVs recovery increased from 10 % for 5 min incubation to 27 % for 25 min
389 incubation, and remained stable even when the incubation time was increased up to 45 min. .
390 For the spiral-formed pattern, the best EVs recovery of 27 % \pm 4 % was thus found for 25 min
391 incubation Under the same incubation time, the U-shaped pattern offered the EVs recovery
392 rate of 39 % \pm 3 %, indicating better interaction between EVs and magnetic beads, and thus
393 higher EVs capture efficiency for the U-shaped pattern. Among the tested droplet movement
394 ones, the straight one gave the least EVs recovery (14 % \pm 4 %) and therefore was not further
395 considered. To obtain more precise information on the quality of the isolated EVs, the
396 samples were analyzed with Particle Metrix' ZetaView [37]. As revealed by Zetaview data
397 (Fig. 4B), 80 % of the recovered EVs fell within the range of the initial size distribution
398 (diameter of 171 nm, accounting for 79 % of the whole population), while the remaining 20 %

399 were represented by larger aggregates (16.7 % for the diameter of 315 nm, and 4.3 % for 472
400 nm). These aggregates are presumably formed due to the PEG capacity to wrap and condense
401 together two or three EVs (corresponding to the sizes of 317 and 472 nm, respectively),
402 making them hard to resuspend in the absence of PEG during the elution step.

403

404 **3.3. Microfluidic droplet-based isolation of EVs from biofluids**

405 The developed microfluidic droplet instrument and protocol were then used to isolate EVs
406 from more complex matrices. First, we used PBS mixed with three matrix proteins, including
407 albumin, IgG and transferrin to imitate human extracellular fluids [38]. This simulated human
408 serum was then spiked with standard EVs (*i.e.*, bovine milk derived EVs at 1.02×10^{11}
409 particles/mL) and passed through the microfluidic droplet system to evaluate the EVs
410 isolation performance. As indicated in Fig. 5, the concentration of collected EVs was $3.69 \times$
411 10^{10} particles/mL, giving an EVs recovery rate of 36 % with spiked simulated human serum,
412 which was not far from that obtained with pure standard EVs (39 %). We then applied the
413 droplet protocol to pony plasma and serum, and compared the results obtained with the in-
414 tube batchwise protocol (Fig. S7 in ESI). When dealing with such complex biofluid matrices,
415 the droplet approach gave an overall particle concentration much higher (up to eight folds)
416 than those obtained with the in-tube method. For instance, with the pony serum sample, the
417 recovered EVs concentration was 8×10^{10} particles/mL when using the microfluidic droplet
418 platform, whereas a significantly lower one (1.05×10^{10} particles/mL) was found for the in-
419 tube method. A similar observation was found for pony plasma, with 17.7×10^{10} particles/mL
420 vs. 4.9×10^{10} particles/mL for microfluidic and in-tube setups, respectively. Moreover, the
421 size distributions of EVs purified with the microfluidic droplet setup are much narrower with
422 only one main peak for each tested sample (Fig. S7). This was, on the other hand, not the case
423 for the in-tube protocol where many peaks were found in the range of 70 - 400 nm for both

424 pony serum and plasma samples. To confirm the identity of EVs isolated from plasma and
425 serum samples, the elution droplets were also analyzed with CE-LIF to reveal different EVs
426 subpopulations (Fig. 6). Based on the peak intensities in each electropherogram, the highest
427 concentration was found for the fraction with the shortest migration time (9-12 min) whereas
428 the signal of the second peak zone (12-15 min) was less intense and this is more remarked for
429 the serum samples. This kind of EVs fingerprints was found similar to those obtained in our
430 previous work with EVs from pony plasma and serum isolated by SEC [28]. Interestingly, the
431 third peak zone (15-20 min) appeared in the electropherograms obtained with both in-batch
432 mode and the droplet system, suggesting that a distinct subpopulation emerges when using the
433 PEG-based isolation methods. Indeed, different isolation methods may lead to the shift or
434 differences in size distributions of the collected EVs, as already evidenced for SEC and UC
435 isolation methods [39, 40]. In our case, the PEG-based method is expected to capture non-
436 selectively all EVs subpopulations, leading to more EVs fractions being visualized with CE-
437 LIF as seen in Fig. 6. NTA measurements for both pony serum and plasma revealed a shift
438 towards smaller size distributions when using the droplet approach (Fig. S7 in ESI). This may
439 correspond to an increased concentration of the small-sized subpopulations, which may
440 correlate to the more pronounced appearance of the third peak zone (15-20 min) in the CE-
441 LIF electropherograms. Nevertheless, no further speculation was made to interpret the
442 presence of these three subpopulations observed by CE as no clear relationship between size
443 and charge properties of EVs and their electrophoretic mobilities can be stated at this stage.

444

445 **4. Conclusion remarks**

446 We successfully developed a new approach (instrumentation and methodology) for EVs
447 isolation from both pre-purified standards and biofluid samples, for the first time in
448 microfluidic droplet format. Using a train of micrometric droplets, containing magnetic beads

449 in the first droplet, the sample, washing and elution solutions in the following ones, we
450 allowed significant sample and reagent volume reduction (by 5 times), minimization of
451 manual operations, diminution of operation time (by twice) and improvement of EVs recovery
452 rate by almost 2 folds. Thanks to automatization and miniaturization that we achieved with
453 droplet microfluidics higher throughput can now be expected. Integration of this microfluidic
454 EVs isolation module as a forefront of downstream EVs analysis and characterization is now
455 envisioned. In the present proof-of-concept study that deals with both instrumental and
456 methodological developments at the same time, the univariate approach was chosen to better
457 understand the impact of the different experimental factors. Indeed, the study on EVs is still at
458 early and emerging stage, and all parameters that would have influence on the EVs stability
459 and behaviour (e.g., morphology modification, surface charge changes, risk of lysis etc.) have
460 not been all identified and mastered, which in turn do not allow simultaneous investigation of
461 multiple variables during the optimization of EVs capture and release. Further optimizations
462 with the multivariate approach could be envisaged in the next phase when all risks of EVs
463 modifications during experiments could be mastered and understood.

464

465

466

467

468

469 **The authors have declared no conflict of interest.**

470

471 **Acknowledgement**

472 This work has been financially supported by the Institut Universitaire de France (for M.
473 Taverna, senior member) and the Agence Nationale de la Recherche (ANR, France) with the

474 grant no. ANR-18-CE29-0005-01. The European fellowship for Lucile Alexandre was
475 supported by the project H2020-MSCA-IF-2019 (IMPED 896313). The doctoral scholarship
476 for Marco Morani was supported by the doctoral school 2MIB (Sciences Chimiques:
477 Molécules, Matériaux, Instrumentation et Biosystèmes) – University Paris Saclay.

478

479

480 **Table 1:** Operation sequence of the microfluidic droplet protocol using droplets of 6 μL each

Operation	Droplet composition	Flowrate ($\mu\text{L/s}$)	Incubation time (min)	Back-and-forth droplet travel distance (+/- μL)
Sample incubation	EVs sample + PEG 5 % (w/v) + magnetic beads (1.5 mg/mL	4	25	6
Washing 1	PEG 5 % / NaCl 0.2 M	0.5	Flush	-
Washing 2	PEG 5 % / NaCl 0.2 M	0.5	Flush	-
Sample elution	PBS 1X	4	5	6

481

482

483

484

485

486

487

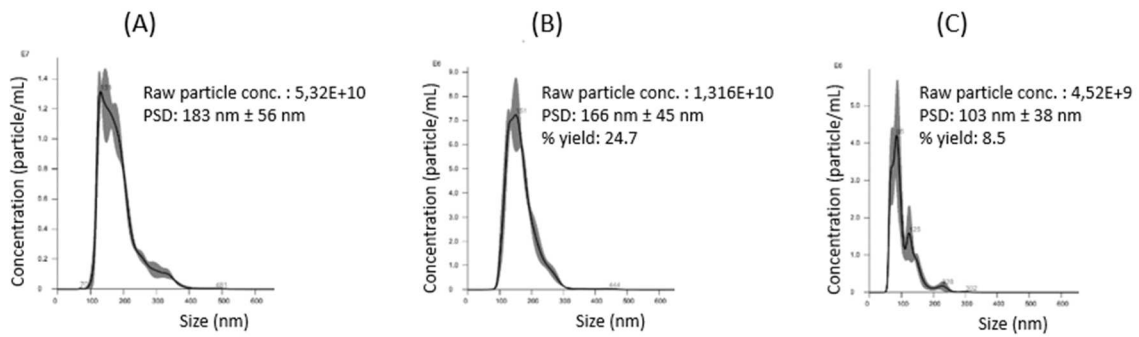
488

489

490

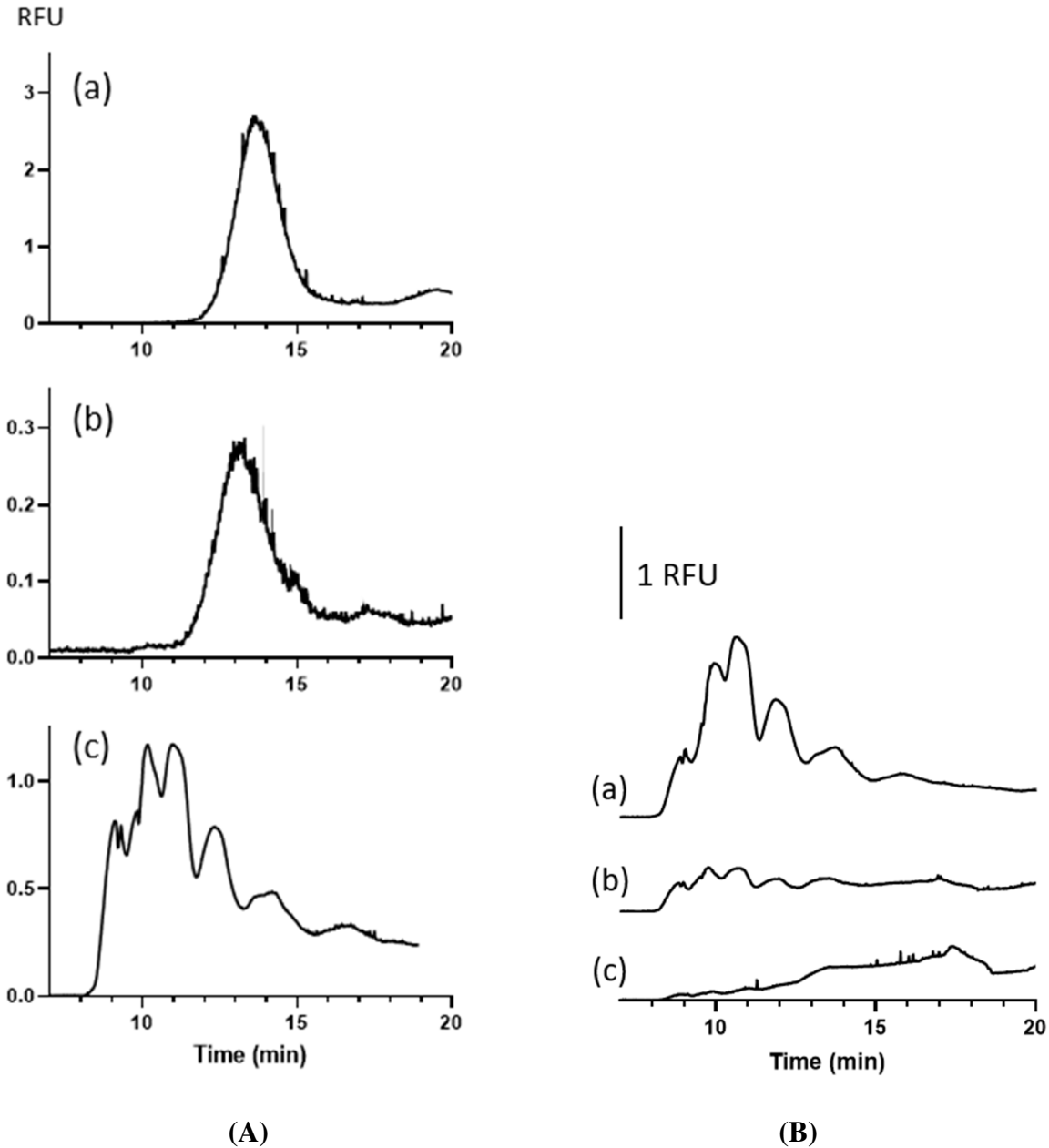
491
492
493
494
495
496
497
498

Figure:



499
500
501
502
503
504
505
506
507
508

Fig. 1. NTA measurements of EVs isolated from bovine milk before purification (A) and after purification with (B) MagExo or (C) ExoCAS-2 method. NTA histograms represent the mean of three replicate measurements of the same sample, with the standard deviation (SD) in grey.



509

510

511

512

513

514

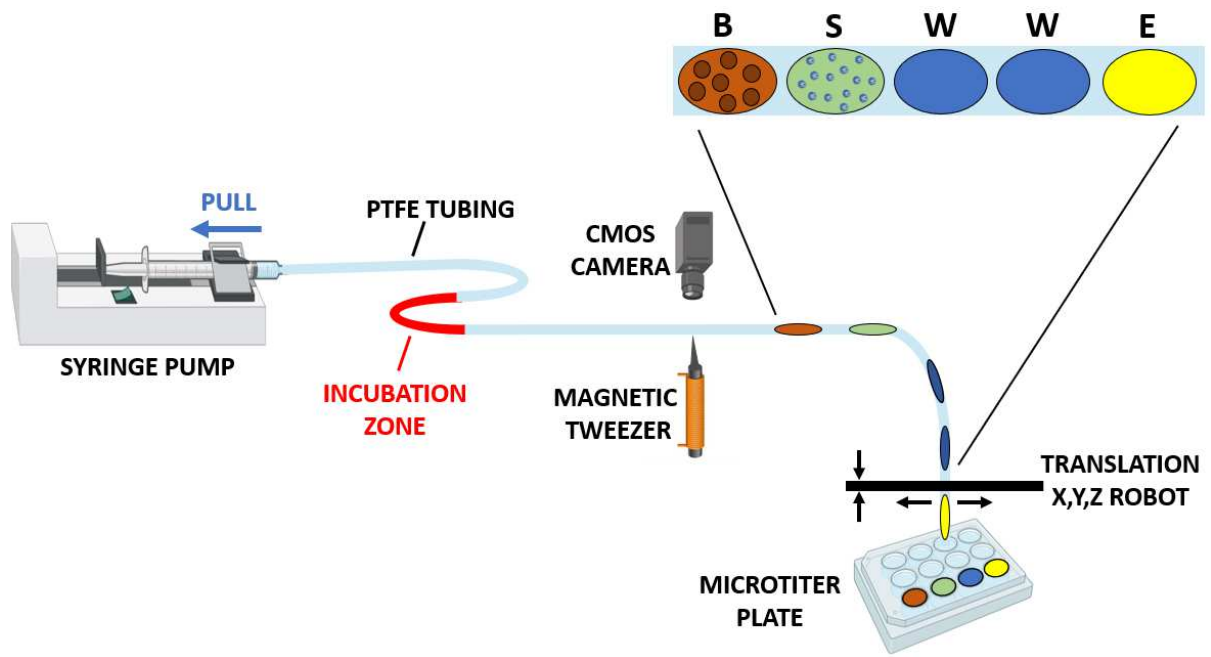
515

516

517

518

Fig. 2. (A) CE-LIF measurements of EVs before purification (a), and after purification with (b) MagExo or (c) ExoCAS-2 method. (B) CE-LIF profiles of solutions of PLL at different concentrations, corresponding to PLL-coated beads suspension volumes of (a) 1 mL; (b) 0.5 mL; (c) 0.1 mL. CE-LIF conditions: fused silica capillary having I.D. of 50 μ m, effective length (L_{eff}) of 50.2 cm and total length (L_{tot}) of 60.2 cm; BGE composed of Tris / CHES (IS 90 mM, pH 8.4); applied voltage: 25 kV (normal polarity).



519

520

521 Fig. 3. Schematic drawing of microfluidic droplet system. B: droplet containing magnetic

522 beads; S: sample droplet; W: washing droplet; E: droplet containing the elution solution.

523 Droplets are separated by oil.

524

525

526

527

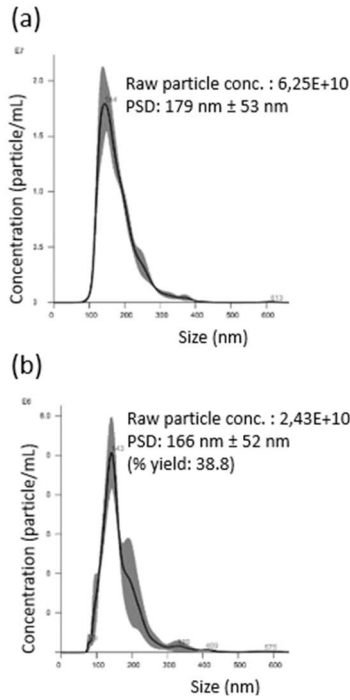
528

529

530

531

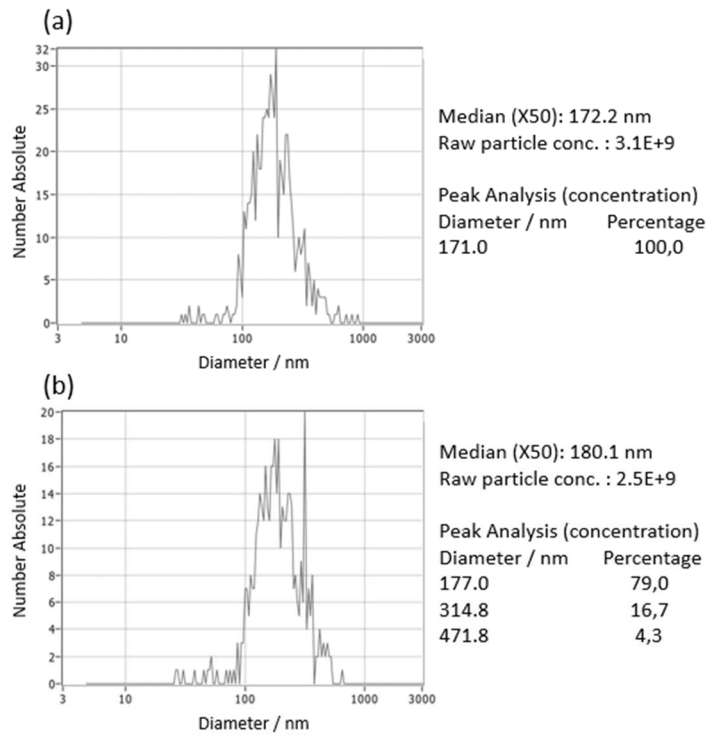
532



533

534

(A)



535

536

(B)

537 Fig. 4. Comparison between (A) Nanosight NS300 (Malvern) vs (B) Zetaview NTA (Particle
538 Metrix) for EVs standard before (a) and after (b) purification with the microfluidic
539 droplet platform using the U-shaped pattern. NTA histograms represent the mean of

540 three replicate measurements of the same sample, with the standard deviation (SD) in
541 grey.

542

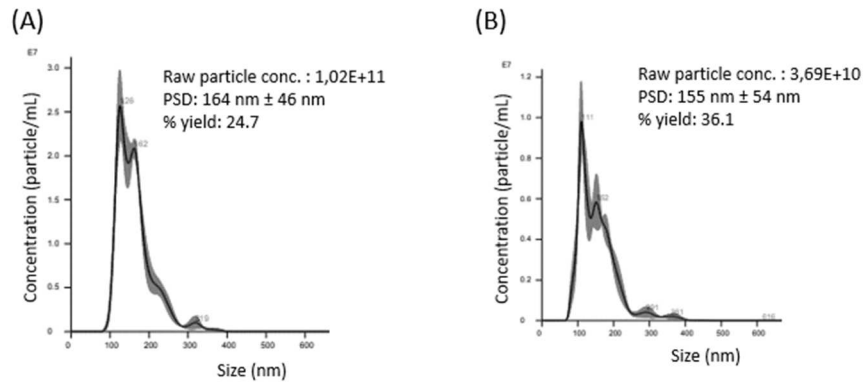
543

544

545

546

547



548

549

550 Fig. 5. NTA measurements of EVs-spiked artificial serum before (A) and after (B) EVs
551 isolation using the microfluidic droplet platform. The sample was 5-time diluted with
552 PBS prior to microfluidic droplet operations. NTA histograms represent the mean of
553 three replicate measurements of the same sample, with the standard deviation (SD) in
554 grey.

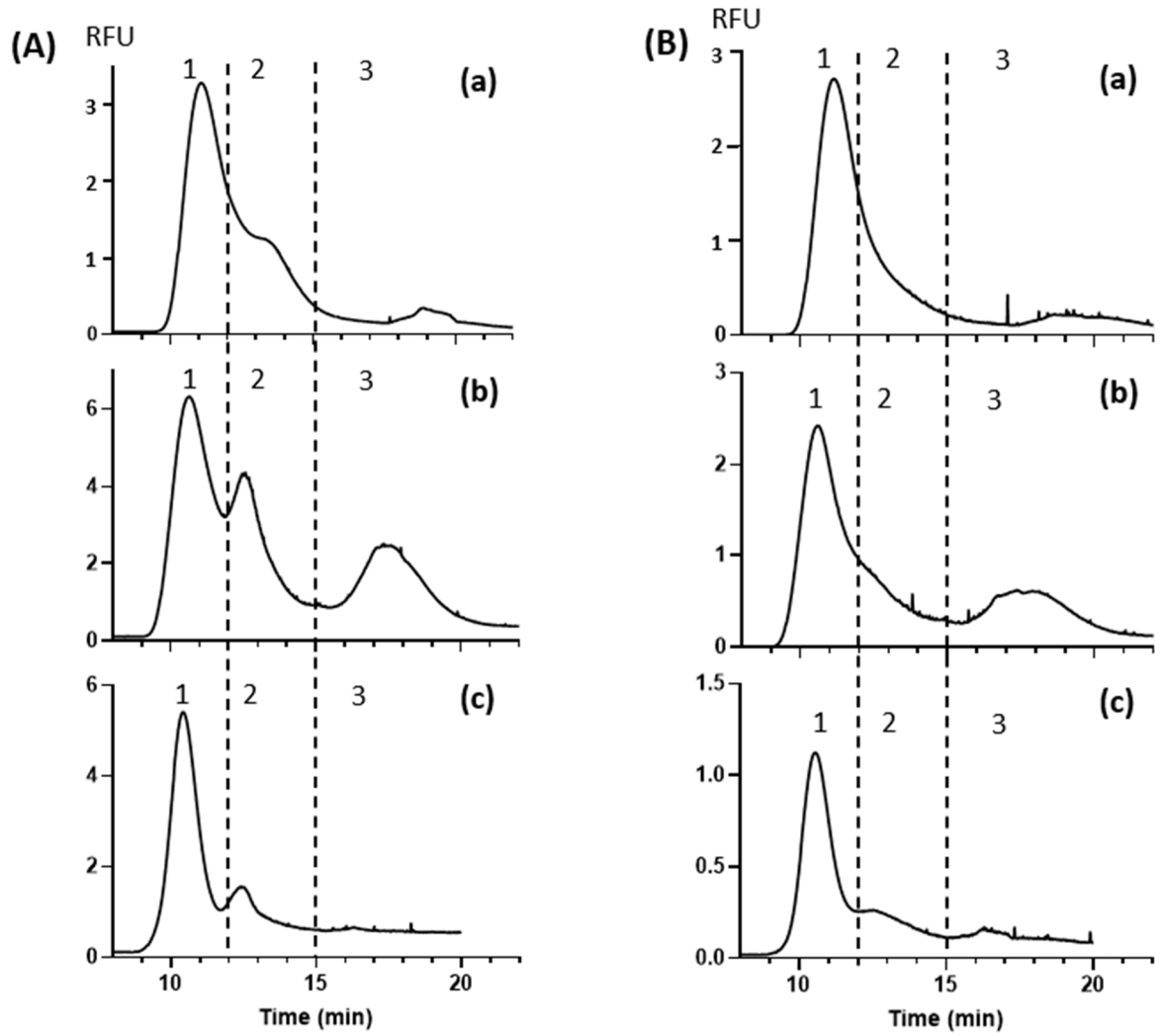
555

556

557

558

559



560

561

562 Fig. 6. CE-LIF for EVs from pony plasma (A) and serum (B), isolated with PEG-based EVs

563 precipitation method in batch mode (a); with the microfluidic droplet system using the

564 U-shaped pattern (b) and isolated with SEC (c). CE conditions as in Fig. 2.

565

566

567

568

569

570

571

572 **References:**

- 573 [1] G. van Niel, G. D'Angelo, G. Raposo, Shedding light on the cell biology of extracellular
574 vesicles, *Nat. Rev. Mol. Cell Biol.* 19(4) (2018) 213-228.
- 575 [2] L.M. Doyle, M.Z. Wang, Overview of extracellular vesicles, their origin, composition,
576 purpose, and methods for exosome isolation and analysis, *Cells* 8(7) (2019) 24.
- 577 [3] J. Howitt, A.F. Hill, Exosomes in the pathology of neurodegenerative diseases, *J. Biol.*
578 *Chem.* 291(52) (2016) 26589-26597.
- 579 [4] W. Guo, Y.B. Gao, N. Li, F. Shao, C.N. Wang, P. Wang, Z.L. Yang, R.D. Li, J. He,
580 Exosomes: New players in cancer, *Oncol. Rep.* 38(2) (2017) 665-675.
- 581 [5] P. Vader, E.A. Mol, G. Pasterkamp, R.M. Schiffelers, Extracellular vesicles for drug
582 delivery, *Adv. Drug Deliv. Rev.* 106 (2016) 148-156.
- 583 [6] H.C. Bu, D.G. He, X.X. He, K.M. Wang, Exosomes: Isolation, analysis, and applications
584 in cancer detection and therapy, *Chembiochem.* 20(4) (2019) 451-461.
- 585 [7] Z. Zhao, H. Wijerathne, A.K. Godwin, S.A. Soper, Isolation and analysis methods of
586 extracellular vesicles (EVs), *Extracellular Vesicles and Circulating Nucleic Acids* 2(1)
587 (2021) 80-103.
- 588 [8] C. Gardiner, D. Di Vizio, S. Sahoo, C. Thery, K.W. Witwer, M. Wauben, A.F. Hill,
589 Techniques used for the isolation and characterization of extracellular vesicles: Results
590 of a worldwide survey, *J. Extracell. Vesicles* 5 (2016).
- 591 [9] M.Y. Konoshenko, E.A. Lekchnov, A.V. Vlassov, P.P. Laktionov, Isolation of
592 extracellular vesicles: General methodologies and latest trends, *Biomed. Res. Int.*
593 (2018) 27.
- 594 [10] H. Yan, Y. Li, S. Cheng, Y. Zeng, Advances in analytical technologies for extracellular
595 vesicles, *Anal. Chem.* 93(11) (2021) 4739-4774.

- 596 [11] T. Liangsupree, E. Multia, M.-L. Riekkola, Modern isolation and separation techniques
597 for extracellular vesicles, *J. Chromatogr. A* 1636 (2021) 461773.
- 598 [12] M. Morani, T.D. Mai, Z. Krupova, G. van Niel, P. Defrenaix, M. Taverna, Recent
599 electrokinetic strategies for isolation, enrichment and separation of extracellular
600 vesicles, *TrAC - Trends Anal. Chem.* (2021) 116179.
- 601 [13] S. Hassanpour Tamrin, A. Sanati Nezhad, A. Sen, Label-free isolation of exosomes using
602 microfluidic technologies, *ACS Nano* (2021).
- 603 [14] Y. Meng, M. Asghari, M.K. Aslan, A. Yilmaz, B. Mateescu, S. Stavrakis, A.J. deMello,
604 Microfluidics for extracellular vesicle separation and mimetic synthesis: Recent
605 advances and future perspectives, *Chem. Eng. J.* 404 (2021) 126110.
- 606 [15] D. Yang, W. Zhang, H. Zhang, F. Zhang, L. Chen, L. Ma, L.M. Larcher, S. Chen, N. Liu,
607 Q. Zhao, P.H.L. Tran, C. Chen, R.N. Veedu, T. Wang, Progress, opportunity, and
608 perspective on exosome isolation - Efforts for efficient exosome-based theranostics,
609 *Theranostics* 10(8) (2020) 3684-3707.
- 610 [16] W.T. Su, H.J. Li, W.W. Chen, J.H. Qin, Microfluidic strategies for label-free exosomes
611 isolation and analysis, *TrAC -Trends Anal. Chem.* 118 (2019) 686-698.
- 612 [17] S.J. Lin, Z.X. Yu, D. Chen, Z.G. Wang, J.M. Miao, Q.C. Li, D.Y. Zhang, J. Song, D.X.
613 Cui, Progress in microfluidics-based exosome separation and detection technologies for
614 diagnostic applications, *Small* 16(9) (2020).
- 615 [18] M. Garcia-Contreras, S.H. Shah, A. Tamayo, P.D. Robbins, R.B. Golberg, A.J. Mendez,
616 C. Ricordi, Plasma-derived exosome characterization reveals a distinct microRNA
617 signature in long duration Type 1 diabetes, *Sci. Rep.* 7 (2017) 10.
- 618 [19] M.N. Madison, J.L. Welch, C.M. Okeoma, Isolation of exosomes from semen for in vitro
619 uptake and HIV-1 infection assays, *Bio-protocol* 7(7) (2017) 21.

- 620 [20] C. Campos-Silva, H. Suárez, R. Jara-Acevedo, E. Linares-Espinós, L. Martínez-Piñeiro,
621 M. Yáñez-Mó, M. Valés-Gómez, High sensitivity detection of extracellular vesicles
622 immune-captured from urine by conventional flow cytometry, *Sci. Rep.* 9(1) (2019) 1-
623 12.
- 624 [21] H. Kim, S. Shin, ExoCAS-2: Rapid and pure isolation of exosomes by anionic exchange
625 using magnetic beads, *Biomedicines* 9(1) (2021) 12.
- 626 [22] X. Fang, C. Chen, B. Liu, Z. Ma, F. Hu, H. Li, H. Gu, H. Xu, A magnetic bead-mediated
627 selective adsorption strategy for extracellular vesicle separation and purification, *Acta*
628 *Biomater.* (2021).
- 629 [23] K. Zhang, Y. Yue, S. Wu, W. Liu, J. Shi, Z. Zhang, Rapid capture and nondestructive
630 release of extracellular vesicles using aptamer-based magnetic isolation, *ACS Sensors*
631 4(5) (2019) 1245-1251.
- 632 [24] D. Brambilla, L. Sola, A.M. Ferretti, E. Chiodi, N. Zarovni, D. Fortunato, M. Criscuoli,
633 V. Dolo, I. Giusti, V. Murdica, EV separation: Release of intact extracellular vesicles
634 immunocaptured on magnetic particles, *Anal. Chem.* 93(13) (2021) 5476-5483.
- 635 [25] C. Liu, X. Xu, B. Li, B. Situ, W. Pan, Y. Hu, T. An, S. Yao, L. Zheng, Single-exosome-
636 counting immunoassays for cancer diagnostics, *Nano Lett.* 18(7) (2018) 4226-4232.
- 637 [26] J. Ko, Y. Wang, K. Sheng, D.A. Weitz, R. Weissleder, Sequencing-based protein
638 analysis of single extracellular vesicles, *ACS Nano* 15(3) (2021) 5631-5638.
- 639 [27] T.D. Mai, D. Ferraro, N. Aboud, R. Renault, M. Serra, N.T. Tran, J.-L. Viovy, C.
640 Smadja, S. Descroix, M. Taverna, Single-step immunoassays and microfluidic droplet
641 operation: Towards a versatile approach for detection of amyloid-beta peptide-based
642 biomarkers of Alzheimer's disease, *Sens. Actuators B* 255 (2018) 2126-2135.

- 643 [28] M. Morani, T.D. Mai, Z. Krupova, P. Defrenaix, E. Multia, M.-L. Riekkola, M. Taverna,
644 Electrokinetic characterization of extracellular vesicles with capillary electrophoresis: a
645 new tool for their identification and quantification, *Anal. Chim. Acta* (2020).
- 646 [29] D. Volodkin, V. Ball, P. Schaaf, J.C. Voegel, H. Mohwald, Complexation of
647 phosphocholine liposomes with polylysine: Stabilization by surface coverage versus
648 aggregation, *Biochim. Biophys. Acta-Biomembr.* 1768(2) (2007) 280-290.
- 649 [30] D. Volodkin, H. Mohwald, J.C. Voegel, V. Ball, Coating of negatively charged
650 liposomes by polylysine: Drug release study, *J. Control. Release* 117(1) (2007) 111-
651 120.
- 652 [31] Y. Takechi, H. Tanaka, H. Kitayama, H. Yoshii, M. Tanaka, H. Saito, Comparative study
653 on the interaction of cell-penetrating polycationic polymers with lipid membranes,
654 *Chem. Phys. Lipids* 165(1) (2012) 51-58.
- 655 [32] A. Gorman, K.R. Hossain, F. Cornelius, R.J. Clarke, Penetration of phospholipid
656 membranes by poly-L-lysine depends on cholesterol and phospholipid composition,
657 *Biochim. Biophys. Acta-Biomembr.* 1862(2) (2020) 10.
- 658 [33] A. Ali-Cherif, S. Begolo, S. Descroix, J.-L. Viovy, L. Malaquin, Programmable magnetic
659 tweezers and droplet microfluidic device for high-throughput nanoliter multi-step
660 assays, *Angew. Chem. Int. Ed.* 51(43) (2012) 10765-10769.
- 661 [34] U. Gündüz, Viscosity prediction of polyethylene glycol–dextran–water solutions used in
662 aqueous two-phase systems, *J. Chromatogr. B* 743(1-2) (2000) 181-185.
- 663 [35] M.A. Stremmer, F.R. Haselton, H. Aref, Designing for chaos: Applications of chaotic
664 advection at the microscale, *Philos. Trans. R. Soc. A-Math. Phys. Eng. Sci.* 362(1818)
665 (2004) 1019-1036.

- 666 [36] D. Bedding, C. Hidrovo, Asme, Investigation of mixing in colliding droplets generated in
667 flow-focusing configurations using laser induced fluorescence, Amer. Soc. Mechanical
668 Engineers, New York, 2016.
- 669 [37] D. Bachurski, M. Schuldner, P.H. Nguyen, A. Malz, K.S. Reiners, P.C. Grenzi, F.
670 Babatz, A.C. Schauss, H.P. Hansen, M. Hallek, E.P. von Strandmann, Extracellular
671 vesicle measurements with nanoparticle tracking analysis - An accuracy and
672 repeatability comparison between NanoSight NS300 and ZetaView, J. Extracell.
673 Vesicles 8(1) (2019).
- 674 [38] J.A. Jaros, P.C. Guest, S. Bahn, D. Martins-de-Souza, Affinity depletion of plasma and
675 serum for mass spectrometry-based proteome analysis, Proteomics for Biomarker
676 Discovery, Springer 2013, pp. 1-11.
- 677 [39] K. Takov, D.M. Yellon, S.M. Davidson, Comparison of small extracellular vesicles
678 isolated from plasma by ultracentrifugation or size-exclusion chromatography: yield,
679 purity and functional potential, J. Extracell. Vesicles 8(1) (2019) 1560809.
- 680 [40] K. Brennan, K. Martin, S. FitzGerald, J. O'Sullivan, Y. Wu, A. Blanco, C. Richardson,
681 M. Mc Gee, A comparison of methods for the isolation and separation of extracellular
682 vesicles from protein and lipid particles in human serum, Sci. Rep. 10(1) (2020) 1-13.
683

